

TRANSIENT WAVES PRODUCED BY A MOVING PRESSURE DISTRIBUTION *

BY

S. L. COLE

Rensselaer Polytechnic Institute

Abstract. This paper provides a theoretical description of the 3-dimensional flow produced by a surface pressure distribution moving in a channel at speeds such that the Froude number based on depth is near 1. The transient flow begins in a fully 3-dimensional manner, then focuses away from the distribution, due to the side walls, into predominantly 2-dimensional “solitary” or “cnoidal” waves. Two sets of these waves are generated continuously by the distribution; one set runs upstream while the other extends downstream.

1. Introduction. This paper grew out of a desire to give a mathematical explanation for the solitary waves produced by Ertekin et al. [4] when they towed a ship model in a tank at Froude numbers (based on depth) near 1. Although trains of solitary waves have been computed as an outcome of several related 2-dimensional problems (see, for example, Akylas [1], Chu et al. [2], Cole [3], Ertekin et al. [4], and Wu and Wu [5]), this derivation is based on a 3-dimensional source.

The asymptotic methods used here show that for small pressure distributions, the transient flow begins by satisfying the classical 3-dimensional linear theory. The free surface then grows with time to become predominantly 2-dimensional away from the disturbance [there satisfying the Korteweg-de Vries (KdV) equation with a forcing term] while remaining fully 3-dimensional only in a small region near the disturbance.

In the following sections, the problem formulation of flow past a pressure distribution is given, the classical linear theory is worked out, and the KdV description of solitary wave generation in the outer region and the quasi-linear 3-dimensional, large time description of flow near the pressure distribution are derived. Numerical computations of the solitary wave generation are presented.

*Received February 27, 1985.

2. Problem formulation. The qualitative results of the experiments of Ertekin et al. can be obtained by modeling the ship as an arbitrarily small pressure distribution moving on the free surface. The coordinate system used is depicted in Figs. 1 and 2.

The mathematical problem is put in nondimensional form by scaling according to the width of the channel and the velocity of the pressure distribution relative to the undisturbed fluid. The important nondimensional parameters are the Froude number F and the pressure strength ε . For this problem, F is taken to be close to 1 and ε is very much less than 1.

Under the assumption that the flow is inviscid, incompressible, and irrotational, the velocity potential Φ satisfies Laplace's equation with boundary conditions along the bottom, sides, and free surface

$$\begin{aligned}\Phi_{xx} + \Phi_{yy} + \Phi_{zz} &= 0, \\ \Phi_z &= 0 \quad \text{on } z = 0, \\ \Phi_y &= 0 \quad \text{on } y = \pm 1, \\ \Phi_z &= \Phi_x \xi_x + \Phi_y \xi_y + \xi_t \quad \text{on } z = h + \xi(x, y, t),\end{aligned}\tag{1}$$

and

$$2\varepsilon\delta(x)\delta(y) + F^2 h \Phi_t + \frac{F^2 h}{2} (\Phi_x^2 + \Phi_y^2 + \Phi_z^2) + z = \frac{F^2 h}{2} + h \quad \text{on } z = h + \xi(x, y, t).$$

Observation of small ship models reveals that for a small time, the free surface is basically undisturbed everywhere except near the pressure distribution. The disturbance grows with time until the free surface exhibits 2-dimensional nonlinear (solitary and cnoidal) waves away from the pressure distribution while remaining fully 3-dimensional only near the

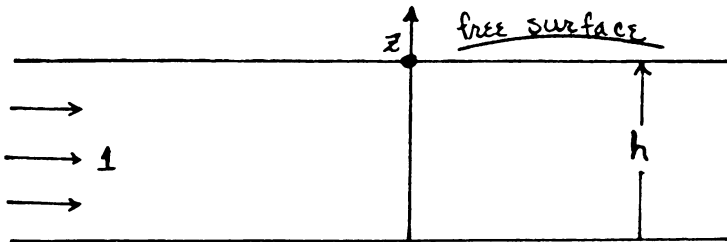


FIG. 1. Side view of coordinate frame fixed with respect to the pressure distribution.

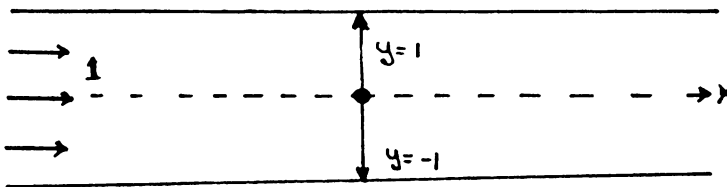


FIG. 2. Top view of coordinate frame fixed with respect to the pressure distribution.

ship. Thus, the mathematical problem can be broken up into three parts. First, classical linear theory can be used to describe the solution everywhere for small time. Second, a predominantly 2-dimensional nonlinear outer solution can be used to describe the free surface away from the pressure distribution for large time. Third, a 3-dimensional quasi-linear inner solution can be used to describe the flow near the distribution for large time.

3. Linear theory. The classical linear theory assumes that Φ and ξ satisfy expansions of the form

$$\Phi = x + \epsilon\theta(x, y, z, t) + \epsilon^2\theta_2(x, y, z, t) + \dots$$

and

$$\xi = \epsilon\eta(x, y, t) + \epsilon^2\eta_2(x, y, t) + \dots,$$

where the order ϵ relations are

$$\begin{aligned} \theta_{xx} + \theta_{yy} + \theta_{zz} &= 0, \\ \theta_z &= 0 \quad \text{on } z = 0, \\ \theta_y &= 0 \quad \text{on } y = \pm 1, \\ \theta_z &= \eta_x + \eta_t \quad \text{on } z = h, \end{aligned} \tag{2}$$

and

$$2\delta(x)\delta(y) + F^2h\theta_t + F^2h\theta_x + \eta = 0 \quad \text{on } z = h.$$

These equations can be solved exactly, giving the free surface solution

$$\begin{aligned} \eta = \sum_{n=0}^{\infty} -\frac{\delta_n}{\pi} \int_{-\infty}^{\infty} e^{-i\kappa x} (\kappa^2 + n^2\pi^2)^{1/2} F^2h \operatorname{ch}(\kappa^2 + n^2\pi^2)_h^{1/2} \\ \cdot \frac{1}{2} \left[\frac{-2\sqrt{} - (\kappa - \sqrt{}) e^{i(\kappa + \sqrt{})t} + (\kappa + \sqrt{}) e^{i(\kappa - \sqrt{})t}}{F^2\kappa^2h \operatorname{ch}(\kappa^2 + n^2\pi^2)_h^{1/2} - (\kappa^2 + n^2\pi^2)^{1/2} \operatorname{sh}(\kappa^2 + n^2\pi^2)_h^{1/2}} \right] d\kappa \cos n\pi y, \end{aligned}$$

where the symbol $\sqrt{}$ denotes the positive root of

$$\sqrt{\frac{(\kappa^2 + n^2\pi^2)^{1/2} \operatorname{sh}(\kappa^2 + n^2\pi^2)_h^{1/2}}{F^2h \operatorname{ch}(\kappa^2 + n^2\pi^2)_h^{1/2}}}$$

and δ_n is the n th Fourier series coefficient of $\delta(y)$ on the interval $-1 \leq y \leq 1$; i.e., $\delta(y) = \sum_{n=0}^{\infty} \delta_n \cos n\pi y$. This integral exists and is continuous for all finite time and all values of the parameter F . However, as t tends toward infinity with $F = 1$, the terms involving y remain bounded while the y -independent term grows, giving

$$\eta \underset{\substack{t \rightarrow \infty \\ F=1}}{\sim} t^{1/3} \frac{1}{2\pi} \int_{-\infty}^{\infty} \exp[-is(x/t^{1/3})] \left[\frac{1 - \exp(is^3h^2/6)}{s^2h^2/3} \right] ds.$$

Thus, the classical linear theory predicts that the given pressure distribution initially produces a 3-dimensional disturbance which grows with time to become asymptotically 2-dimensional when F is near 1.

4. Outer solution. The linear theory suggests that the solution away from the pressure distribution satisfies an asymptotic expansion in which the x and t variables are large compared to the y and z variables, the flow is predominantly 2-dimensional, and the free surface height is larger than order ε . These ideas are captured in the outer theory by using the stretched coordinates $\tilde{x} = \varepsilon^{1/3}x$ and $\tilde{t} = \varepsilon t$ with $F^2 = 1 + \varepsilon^{2/3}K$ and the expansions

$$\Phi = x + \varepsilon^{1/3} \left[f_1(\tilde{x}, \tilde{t}) + \varepsilon^{2/3} f_2(\tilde{x}, \tilde{t}) - \frac{z^2}{2!} f_{1\tilde{x}\tilde{x}}(\tilde{x}, \tilde{t}) + \varepsilon^{4/3} \left(f_3(\tilde{x}, \tilde{t}) - \frac{z^2}{2!} f_{2\tilde{x}\tilde{x}}(\tilde{x}, \tilde{t}) + \frac{z^4}{4!} f_{1\tilde{x}\tilde{x}\tilde{x}\tilde{x}}(\tilde{x}, \tilde{t}) + G(\tilde{x}, y, z, \tilde{t}) \right) + \dots \right]$$

and $\xi = \varepsilon^{2/3}\tilde{\eta}(\tilde{x}, \tilde{t}) + \varepsilon^{4/3}\tilde{\eta}_2(\tilde{x}, y, \tilde{t}) + \dots$. The exact scaling used is the distinguished limit of the general expansion of this form.

By substituting these expansions into Eq. (1), it is found that $\tilde{\eta}$ must satisfy the KdV equation

$$2\tilde{\eta}_t = \frac{3\tilde{\eta}\tilde{\eta}_{\tilde{x}}}{h} - K\tilde{\eta}_{\tilde{x}} + \frac{h^2}{3}\tilde{\eta}_{\tilde{x}\tilde{x}\tilde{x}} + \delta'(\tilde{x}). \quad (3)$$

This is exactly the same equation found in the far field of flow past a small bump [3].

The outer solution matches the linear solution in an intermediate region as the outer variables \tilde{x} and \tilde{t} tend to zero and the linear variables x and t tend to infinity. This intermediate region is defined along similarity curves in terms of the variables

$$\bar{x} = \left(\frac{\varepsilon}{\gamma} \right)^{1/3} x = \frac{\tilde{x}}{\gamma^{1/3}} \quad \text{and} \quad \bar{t} = \left(\frac{\varepsilon}{\gamma} \right) t = \frac{\tilde{t}}{\gamma} \quad \text{with} \quad \gamma \xrightarrow{\varepsilon \rightarrow 0} 0 \quad \text{and} \quad \left(\frac{\gamma}{\varepsilon} \right) \xrightarrow{\varepsilon \rightarrow 0} \infty.$$

Since the linear free surface $\xi = \varepsilon\eta(x, t) + \dots$ must match the nonlinear outer free surface $\xi = \varepsilon^{2/3}\tilde{\eta}(\tilde{x}, \tilde{t}) + \dots$, this implies that $\tilde{\eta}(\tilde{x}, \tilde{t})$ tends to zero as \tilde{t} tends to zero.

If one considers $\tilde{t} \rightarrow 0$ and neglects the term $\tilde{\eta}\tilde{\eta}_{\tilde{x}}$ in (3), then the remaining terms must satisfy the relation

$$2\tilde{\eta}_t = -K\tilde{\eta}_x + \frac{h^2\tilde{\eta}}{3}l_{\tilde{x}\tilde{x}\tilde{x}} + \delta'(\tilde{x}),$$

which has the solution

$$\tilde{\eta}_t = \frac{1}{2\pi} \int_{-\infty}^{\infty} e^{-i\kappa\tilde{x}} \left[\frac{1 - \exp(1/2(i\kappa K + i\kappa^3 h^2/3)\tilde{t})}{K + \kappa^2 h^2/3} \right] dk.$$

In terms of the intermediate variables, this becomes

$$\tilde{\eta}_t \sim_{\varepsilon \rightarrow 0} \gamma^{1/3} \bar{t}^{1/3} \cdot \frac{1}{2\pi} \int_{-\infty}^{\infty} \exp[-is(\bar{x}/\bar{t}^{1/3})] \left[\frac{1 - \exp(is^3 h^2/6)}{s^2 h^2/3} \right] ds,$$

while the linear solution becomes

$$\eta \sim_{\varepsilon \rightarrow 0} \left(\frac{\gamma}{\varepsilon} \right)^{1/3} \bar{t}^{1/3} \cdot \frac{1}{2\pi} \int_{-\infty}^{\infty} \exp[-is(\bar{x}/\bar{t}^{1/3})] \left[\frac{1 - \exp(is^3 h^2/6)}{s^2 h^2/3} \right] ds.$$

Thus $\varepsilon^{2/3}\tilde{\eta}_t(\bar{x}, \bar{t}) \sim_{\varepsilon \rightarrow 0} \varepsilon\eta(\bar{x}, \bar{t})$ and the solutions match.

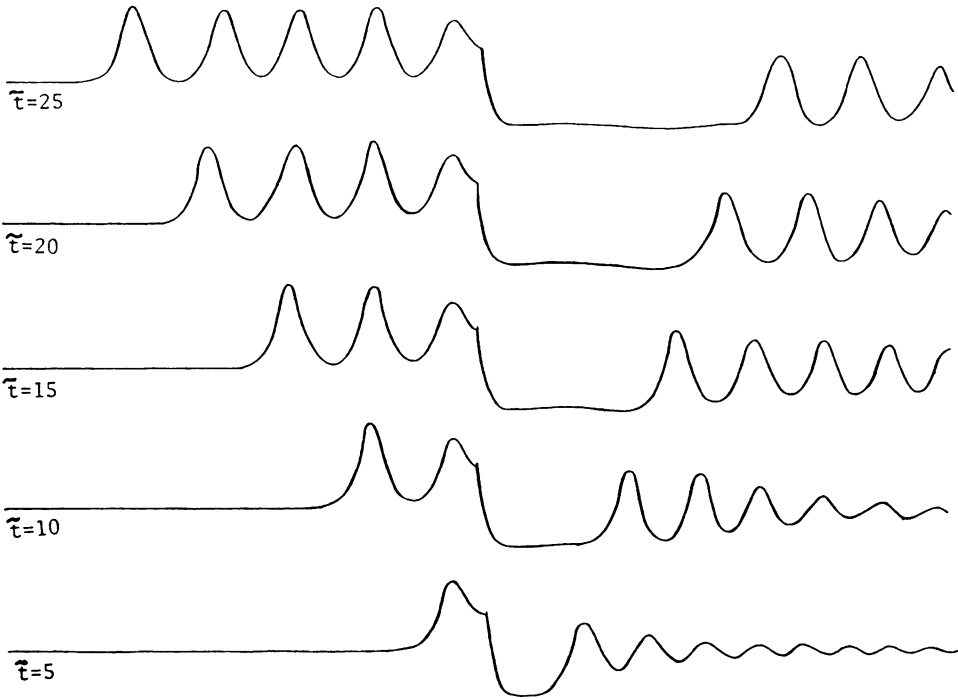


FIG. 3. Computed free surface for $K = 0$ ($F = 1$).

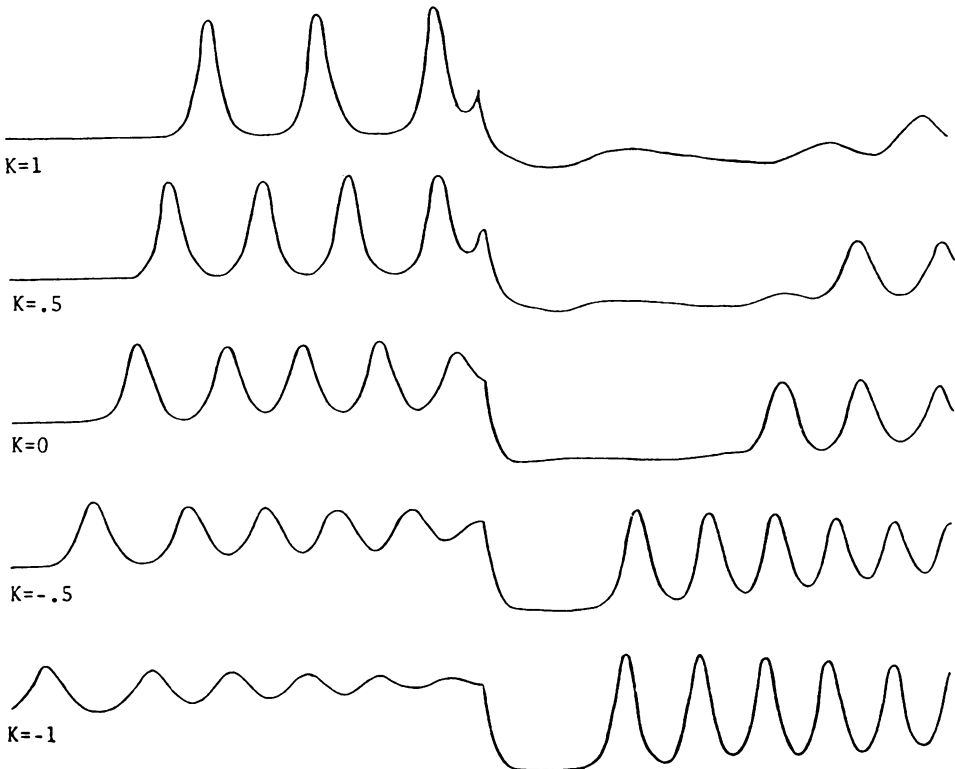


FIG. 4. Computed free surface for $K = -1, -0.5, 0, 0.5$, and 1 with $\tilde{t} = 25$.

When computed numerically, Eq. (3) produces a periodic train of solitary waves which run upstream. The free surface computations presented in Figs. 3 and 4 are a copy of those given in [3]. Although Ertekin et al. observed experimentally that these waves break for Froude numbers far enough away from 1, breaking cannot be predicted from this theory.

In order to obtain the above results, it is not necessary to assume that the pressure distribution is defined by the product of delta functions. It can be shown that all pressure distributions with arbitrary shape $f(x, y)$, where $f(x, y) = \sum_{n=0}^{\infty} f_n(x) \cos n\pi y$ and $\int_{-\infty}^{\infty} f_0(x) dx = 1/2$, have the same asymptotic behavior in the far field. Thus, all such pressure distributions appear in the far field to have been produced by a product of delta functions. The actual shape of the pressure distribution affects only the flow near the distribution.

5. Inner solution. The classical linear solution is valid for small time, $t \sim_{\epsilon \rightarrow 0} o(\epsilon^{-1})$, and all x . The outer solution is valid for large time, $t \sim_{\epsilon \rightarrow 0} O(\epsilon^{-1})$, far away from the disturbance, $x \sim_{\epsilon \rightarrow 0} O(\epsilon^{-1/3})$. The solution near the pressure distribution, $x \sim_{\epsilon \rightarrow 0} o(\epsilon^{-1/3})$, for large time, $t \sim_{\epsilon \rightarrow 0} O(\epsilon^{-1})$, completes the description and is given next.

The inner solution must match the outer solution as the outer variable \tilde{x} tends to zero. As $\tilde{x} \rightarrow 0$, the outer solution takes the form

$$\begin{aligned} \Phi \underset{\tilde{x} \rightarrow 0}{\sim} & x + \epsilon^{1/3} f_1(0, \tilde{t}) + \epsilon^{2/3} x f_{1,\xi}(0, \tilde{t}) + \epsilon \tilde{H}(x, y, z, \tilde{t}) + \dots \\ & = x \left(1 - \epsilon^{2/3} \frac{\tilde{\eta}(0, \tilde{t})}{h} \right) + \epsilon^{1/3} f_1(0, \tilde{t}) + \epsilon \tilde{H}(x, y, z, \tilde{t}) + \dots \end{aligned}$$

with $\xi \sim_{\tilde{x} \rightarrow 0} \epsilon^{2/3} \tilde{\eta}(0, \tilde{t}) + \epsilon \tilde{\xi}(x, y, \tilde{t}) + \dots$.

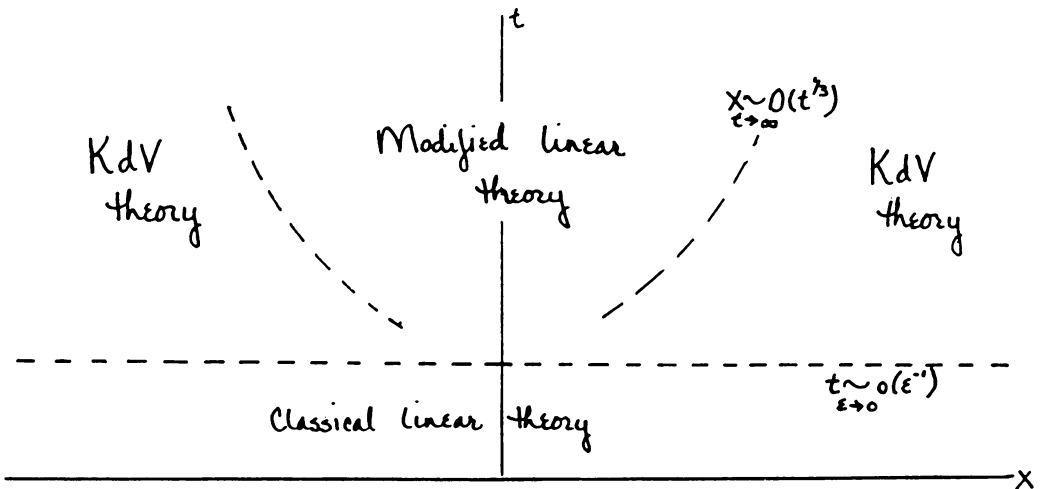


FIG. 5. Regions of validity for the classical linear theory, KdV, and modified linear theories.

The local flow has velocity $U_l = 1 - \varepsilon^{2/3}\tilde{\eta}(0, \tilde{t})/h$, height $h_l = h + \varepsilon^{2/3}\tilde{\eta}(0, \tilde{t})$, and Froude number squared $F_l^2 \sim_{\varepsilon \rightarrow 0} F^2(1 - 3\varepsilon^{2/3}\tilde{\eta}(0, \tilde{t})/h)$. Since the numerical computations show that $\tilde{\eta}(0, \tilde{t}) > 0$ for all $\tilde{t} > 0$ with $F \equiv 1$ and the computations are continuous as a function of the parameter F , the flow near the distribution is subcritical for all F sufficiently close to 1. This allows a modified linear theory to be defined using local parameters and the asymptotic expansion

$$\Phi = U_l x + \varepsilon^{1/3} f_1(0, \tilde{t}) + \varepsilon H(x, y, z, \tilde{t}) + \dots$$

with the free surface located at

$$z = h_l + \varepsilon \zeta(x, y, \tilde{t}) + \dots$$

H and ζ satisfy the order ε relations

$$\begin{aligned} H_{xx} + H_{yy} + H_{zz} &= 0, \\ H_z &= 0 \quad \text{on } z = 0, \\ H_y &= 0 \quad \text{on } y = \pm 1, \\ H_z &= U_l \zeta_x \quad \text{on } z = h_l, \end{aligned}$$

and

$$2\delta(x)\delta(y) + \frac{F_l^2 h_l}{U_l} H_x + \zeta = 0 \quad \text{on } z = h_l.$$

The free surface solution is

$$\zeta = \sum_{n=0}^{\infty} \frac{\delta_n}{\pi} \int_{-\infty}^{\infty} e^{-i\kappa x} \left[\frac{(\kappa^2 + n^2\pi^2)^{1/2} \text{sh}[(\kappa^2 + n^2\pi^2)^{1/2} h_l]}{F_l^2 h_l \kappa^2 \text{ch}[(\kappa^2 + n^2\pi^2)^{1/2} h_l] - (\kappa^2 + n^2\pi^2)^{1/2} \text{sh}[(\kappa^2 + n^2\pi^2)^{1/2} h_l]} \right] dk \cdot \cos n\pi y + c \sin \kappa^* x \text{ch} \kappa^* h_l$$

where the symbol f denotes the Cauchy principal value, κ^* is the positive root of $F_l^2 h_l \kappa \text{ch} \kappa h_l - \text{sh} \kappa h_l = 0$, and c is an arbitrary function of \tilde{t} which is determined by matching to the outer solution.

The outer solution matches the inner solution in an intermediate region as the outer variable \bar{x} tends to zero and the inner variable x tends to infinity. This intermediate region can be defined in terms of the variable $\bar{x} = (\varepsilon/\gamma)^{1/3} x = \bar{x}/\gamma^{1/3}$, where $(\gamma/\varepsilon) \rightarrow_{\varepsilon \rightarrow 0} \infty$ and $\gamma \rightarrow_{\varepsilon \rightarrow 0} 0$. In this region, the outer solution places the free surface at

$$z \underset{\bar{x} \rightarrow 0}{\sim} h + \varepsilon^{2/3} \tilde{\eta}(0, \tilde{t}) + \bar{x} \varepsilon^{2/3} \gamma^{1/3} \begin{cases} \tilde{\eta}_{\bar{x}}(0^+, \tilde{t}) & \text{for } \bar{x} > 0^+ \\ \tilde{\eta}_{\bar{x}}(0^-, \tilde{t}) & \text{for } \bar{x} < 0 \end{cases}$$

[†] There is a jump in the slope of $\tilde{\eta}$ at $\bar{x} = 0$ of $(\tilde{\eta}_{\bar{x}}(0^+) - \tilde{\eta}_{\bar{x}}(0^-)) = -3/h^2$ due to the presence of the term $\delta'(\bar{x})$ in the differential equation defining $\tilde{\eta}$,

$$2\tilde{\eta}_t = \frac{3\tilde{\eta}\tilde{\eta}_{\bar{x}}}{h} - K\tilde{\eta}_{\bar{x}} + \frac{h^2}{3}\tilde{\eta}_{\bar{x}\bar{x}\bar{x}} + \delta'(\bar{x}). \tag{3}$$

while the inner solution assumes the form

$$z \underset{|x| \rightarrow \infty}{\sim} h + \varepsilon^{2/3} \tilde{\eta}(0, \tilde{t}) + \varepsilon \frac{\delta_0}{\pi} \int_{-\infty}^{\infty} e^{-i\kappa x} \left[\frac{\text{sh } \kappa h_l}{F_l^2 h_l \kappa \text{ch } \kappa h_l - \text{sh } \kappa h_l} \right] d\kappa + \varepsilon c \sin \kappa^* x \text{ch } \kappa^* h_l$$

$$\underset{|x| \rightarrow \infty}{\sim} h + \varepsilon^{2/3} \tilde{\eta}(0, \tilde{t}) + \bar{x} \varepsilon^{2/3} \gamma^{1/3} \left(\frac{-3}{2h^2} \text{sign } \bar{x} + c\kappa^* \right).$$

By choosing $c\kappa^* = (3/2h^2) + \tilde{\eta}_{\bar{x}}(0^+, \tilde{t})$, the solutions match.

6. Remarks. It is interesting to note that solitary waves were generated experimentally in qualitatively the same fashion over a range of Froude numbers between 0.2 and 1.2. Thus, it appears that the above ideas predict reasonable results even for values of ε which are not arbitrarily small.

Acknowledgment. I wish to thank Professors Wu and Wehausen for their descriptions of experimental work and for pointing out related numerical computations made by their groups and Professor Akylas. The numerical computations presented here were made at the Seaver Computer Center of Pomona College.

REFERENCES

- [1] T. R. Akylas, *On the excitation of long nonlinear water waves by a moving pressure distribution*, J. Fluid Mech. **141**, 455–466 (1984)
- [2] C. K. Chu, L. W. Xiang, and Y. Baransky, *Solitary waves induced by boundary motion*, Comm. Pure Appl. Math. **36**, 495–504 (1983)
- [3] S. L. Cole, *Transient waves produced by flow past a bump*, Wave Motion **7**, 579–587 (1985)
- [4] R. C. Ertekin, W. C. Webster, and J. V. Wehausen, *Ship-generated solitons*, Proc. 15th Sympos. Naval Hydrodynamics, In press.
- [5] D.-M. Wu and T. Y. Wu, *Three-dimensional nonlinear long waves due to moving surface pressure*, Proc. 14th Sympos. Naval Hydrodynamics, National Academy Press, Washington, D. C., pp. 103–125, 1983